STUDY OF THE $pp \to d\pi^+$ REACTION CLOSE TO THE THRESHOLD*

S. FÖRTSCH

Institut für Kernphysik, Forschungszentrum Jülich
Jülich, Germany**
for the GEM collaboration

(Received October 9, 1996)

M. Drochner [b]†, J. Ernst [g], L. Freindl [d], D. Frekers [h], W. Garske [h], M. Hawash [a]‡, S. Igel [a], R. Jahn [g], L. Jarczyk [c], G. Kemmerling [b], K. Kilian [a], S. Kliczewski [d], W. Klimala [c], D. Kolev [f], T Kutsarova [e], G. Lippert [a], H. Machner [a], R. Maier [a], C. Nake [a], B. Razen [a], P. von Rossen [a], K. Scho [g], R. Siudak [d], J. Smyrski [c], A. Strzałkowski [c], R. Tsenov [f], P. A. Żołnierczuk [a,c], K. Zwoll [b]

[a] Institut für Kernphysik, Forschungszentrum Jülich, Germany
[b] Zentrallabor für Elektronik, Forschungszentrum Jülich, Germany
[c] Institute of Physics, Jagellonian University, Kraków, Poland
[d] Institute of Nuclear Physics, Kraków, Poland
[e] Institute of Nuclear Physics and Nuclear Energy, Sofia, Bulgaria
[f] Physics Faculty, University of Sofia, Bulgaria
[g] Institut für Strahlen- und Kernphysik der Universität Bonn, Germany
[h] Institut für Kernphysik, Universität Münster, Germany

The $pp \to d\pi^+$ reaction is studied at excess energies between 0.275 MeV and 3.86 MeV. Differential and total cross sections were measured employing a magnetic spectrometer with an acceptance of close to 4π in the center of mass system. From the total cross sections the S and P–wave contributions are deduced. The measured anisotropies between 0.008 and 0.29 suggest a non–negligible P–wave contribution even close to threshold. Compared to existing data the present results offer no evidence for charge–symmetry breaking or time reversal violation.

PACS numbers: 13.60. Le

* Presented at Meson-96 Workshop, Cracow, Poland, 10–14 May, 1996.
** also at National Accelerator Centre, Faure, South Africa.
† also at TU Dresden, Dresden, Germany.
‡ on leave of absence from Nuclear Research Centre, A. E. A., Cairo, Egypt

1. Introduction

Since the postulation and discovery of the pion about sixty years ago, meson exchange processes have facilitated the understanding of the interaction between two nucleons. Especially the radial dependence of these processes has played a crucial part in describing the long and short range attractive part of the nucleon–nucleon (NN) potential. A major aim of intermediate-energy physics is therefore the understanding of the production and absorption of pions in NN interactions. Problems experienced with the interaction of low-energy pions with nuclei arise from the lack of an understanding of the process involving reactions with pions. Before such questions of pion–nucleus reactions can be addressed, pion production in such elementary reactions as *e.g.* the $pp \to d\pi^+$ reaction must be understood. The other elementary pion production reactions are:

$$\begin{aligned} &pp \to pn\pi^+ \\ &pp \to pp\pi^0 \\ &pn \to d\pi^0 \\ &pn \to pp\pi^- \\ &pn \to pn\pi^0 \\ &pn \to nn\pi^+ \end{aligned}$$

From both an experimental and theoretical point of view there is a preference for the reaction $pp \to d\pi^+$ in studying pion production near the threshold. This reaction is the simplest to measure as it is induced by a charged particle and leads to two charged particles in the final state according to two–body kinematics. Theoretical analyses also benefit from this reaction at low energies as there are only three transition possibilities as far as angular momentum conservation is concerned:

$$\begin{aligned} 2p(^3P_1) &\to d(^3S_1) + \pi^+ \text{ in } S\text{-state} \\ 2p(^1D_2) &\to d(^3S_1) + \pi^+ \text{ in } P\text{-state} \\ 2p(^1S_0) &\to d(^3S_1) + \pi^+ \text{ in } P\text{-state} \end{aligned}$$

More than these three possibilities apply however for the cases where the two nucleons in the exit channel are left unbound. Apart from this reaction chosen in the present study for the above reasons, the other pion–production routes have also attracted recent interest. Reactions leading to threshold meson production are characterized by large momentum transfer ($\sim$ 370 MeV/c in the present reaction) and dominant S–wave in the exit channel. Both these processes can be described in terms of heavy meson exchange. Horowitz [1] introduced a meson exchange current (MEC) term in addition to single pion emission and pion rescattering in order to enhance the S–wave production. This additional mechanism also accounts for a lower cross section when modern form factors for the π–NN interaction are applied. His results are consistent with findings from $pp \to pp\pi^0$ measurements [2, 3]. These recent calculations and interpretations however exclude the reaction of this study but were performed on data from the $np \to d\pi^0$ reaction [4] and the time–reversed reaction [5] $\pi^+d \to pp$. Due to uncertainties in the Coulomb correction applied to the last mentioned reaction, comparisons with the data from the isospin–related reaction at small pion momenta are found to be doubtful [4]. Most recently Niskanen [6] showed in his calculations and in particular for the present reaction that MEC contributions are negligible compared to the S–wave cross section which originates from P–wave pions decaying from the Δ isobar and subsequently rescattering off the second nucleon.

2. Motivation

Based on the barrier penetration model, the Gell–Mann and Watson parameterization [7] of the total cross section near threshold can be written as:

$$\sigma(pp \to d\pi^+) = \alpha_0\eta + \alpha_1\eta^3\,, \qquad (1)$$

where η is the c.m. pion momentum divided by its rest mass. Results from the charged and uncharged particle induced reactions yield S–wave cross section rates of $\alpha_0 = 0.24$ mb [5] and 0.184 mb [4], respectively. This discrepancy was partially reduced by the recent data [8] for the $\pi^+d \to pp$ reaction in the range $0.215 \leq \eta \leq 0.518$. It has to be noted that the neutron induced reaction only covers the pion momentum range up to $\eta = 0.32$ where the S–wave contribution to the total cross section is believed to dominate, whereas the other data sets are mostly dominated by P–wave contributions. The aim of the present study was therefore to measure differential and total cross sections for the $pp \to d\pi^+$ reaction close to the threshold ($\eta \leq 0.22$) making use of almost 4π detector acceptance in the c.m. system. No complete angular distributions for this reaction in the present η range existed prior to our measurements.

3. Experiment

The experiment was performed at COSY (COoler SYnchrotron) in Jülich at five different proton beam momenta between 789.75 MeV/c and 800.5 MeV/c. These correspond to excess energies of between 0.275 MeV and 3.36 MeV, respectively. Proton beams were focussed onto the target point of a 3Q2DQ magnetic spectrometer. Acceptances of the spectrometer are ±25 mrad in the horizontal or x–direction and ±100 mrad in the vertical or y–direction and ±4.5% with regard to the central value of the chosen momentum bite. The beam spot had dimensions of less than 2 mm and 1 mm (FWHM) and divergences of 1.8 mrad and 3.8 mrad in the x– and y–direction respectively. Its momentum spread was measured to be $\Delta p/p = 4 \times 10^{-4}$ and it had a duty factor of 10%. The target was a cell [9] containing liquid hydrogen, with a 6–mm–diameter and a thickness of 4.4 ± 0.2 mm for the 800.5 MeV/c run and 2.2 ± 0.1 mm for the other runs. Mylar windows were of 2 μm thickness each. In order to suppress beam–halo events, an annular plastic scintillator with a 3–mm–diameter inner hole was used in front of the target cell as a veto counter.

The deuteron tracks were determined in the focal plane of the spectrometer with two stacks of multi–wire drift chambers (MWDC) which allow position measurements both in the horizontal and vertical direction. A track resolution of 0.2 mm was achieved. The spectrometer operated in the point–to–parallel mode in the vertical direction and in the dispersive image mode in the horizontal direction. The magnetic field for a central momentum corresponded approximately to the mean momentum of the recoiling deuterons. The deuteron ejectiles had momenta up to 775.4 MeV/c and emission angles up to 40 mrad. Under these conditions the beam protons caused an extensive background in the focal plane due to the similar magnetic rigidities between the protons and deuterons. These background events were suppressed to a large extent as follows: The MWDC stacks were followed by a timing detector consisting of four layers of scintillator paddles. By using pulse–height discrimination on the signals from the first layer, the number of recorded protons was reduced. An aluminum absorber with a thickness sufficient to stop the deuterons was mounted between the third and fourth layer. While the first three layers operated in coincidence, the detectors in the last layer served as a veto counter. Coincident pion events from the reaction were also included in the trigger by using an annular plastic scintillator with a 5–mm–diameter hole located behind the target. The pion detector and the scintillators of the third layer served as delayed stop and start detectors respectively for a time–of–flight (TOF) measurement over a flight path of ~18 m through the spectrometer. For the measurements at the four lower beam momenta, the pion trigger was removed from the event trigger to allow for the reduction in the momentum phase space distribution of the pions as the beam momentum decreases. In this case the TOF information was obtained from the timing signals of the second and third layer separated by ~2.5m. A permissible intensity of 5×10^6 protons per spill limited the total event rate. At this rate there was no measurable dead time in the fast trigger system nor in the data acquisition system.

4. Results

Momentum vectors of the recoiling deuterons at the target were reconstructed from the measured tracks in the focal plane. The momentum distribution as obtained from the raw data is shown in the upper part of Fig. 1. In order to reduce the background events further, the following constraints were applied to the data in the off-line analysis: a gate was set around the deuterons in the TOF spectrum. Remaining background was rejected by applying a gate with a width of four times the experimental resolution on the reconstructed pion mass. The resulting deuteron-momentum distribution is shown in the lower part of Fig. 1. In order to obtain c.m. angular distributions, the ellipsoidal momentum distributions in the lab system were transformed into the spherical c.m. distributions and then projected onto

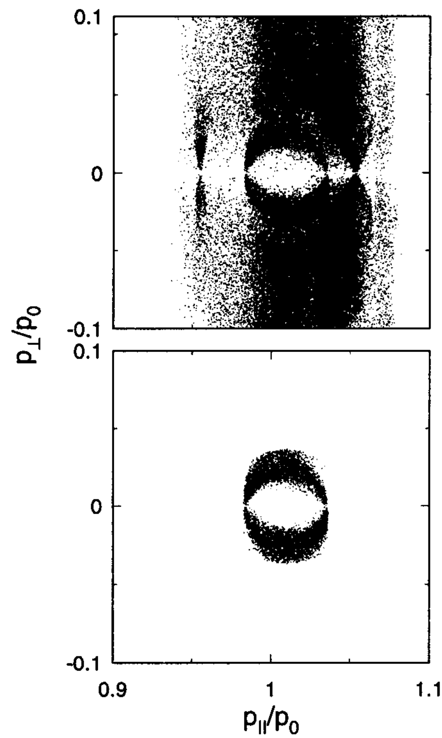

Fig. 1. Density distributions of the deuteron ejectiles as a function of momentum parallel ($p_{||}$) and perpendicular ($p_\perp$) to the beam direction, normalized to the central momentum of the magnetic spectrometer set to p_0 = 730 MeV/c. Raw data as obtained on-line are shown in the upper part. Same data obtained after applying constraints off-line as discussed in the text are shown in the lower part.

the momentum axis parallel to the beam direction ($p_{||}$) which corresponds to an integration over the azimuthal scattering angle. Deuteron data measured at the highest beam momentum were severely affected in the low momentum range by the detector acceptance limits and were therefore excluded from the present study.

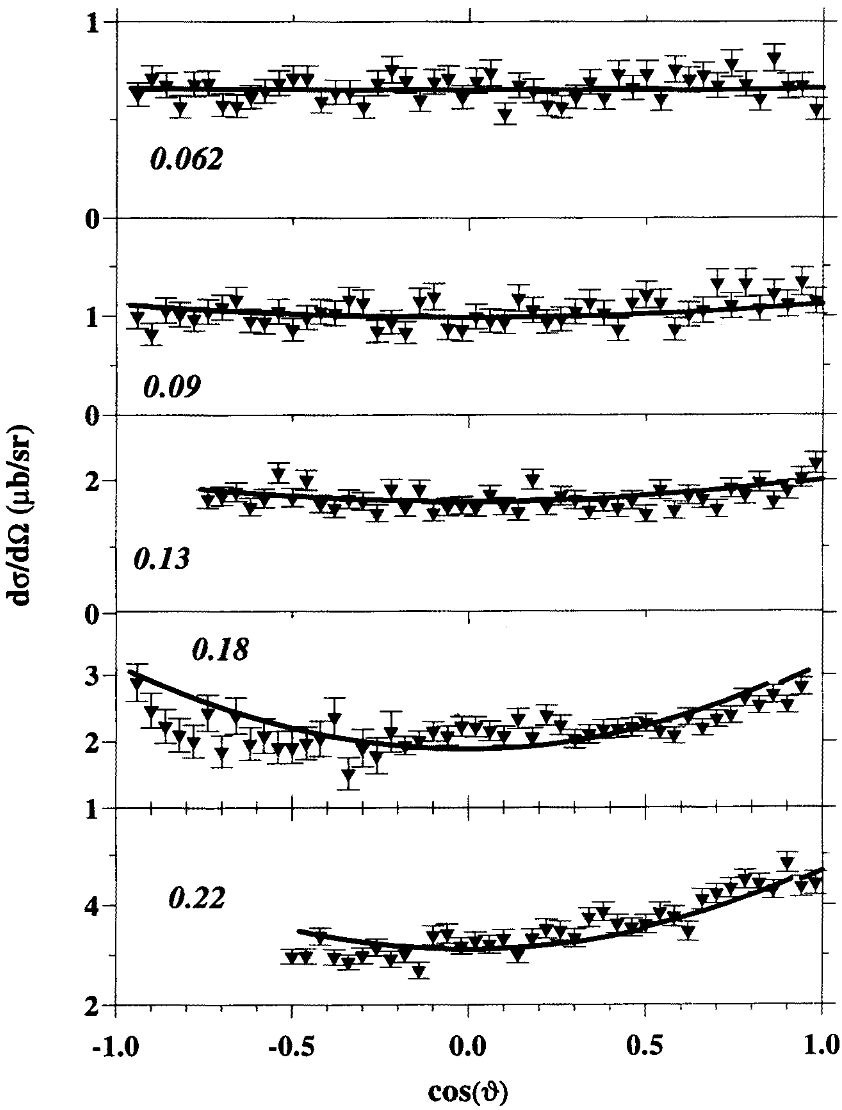

Fig. 2. Measured c.m. differential cross sections at five different beam momenta indicated by the number in terms of η. Legendre polynomial fits are shown as curves.

Differential cross sections were extracted by normalizing the angular distribution yields to target thickness and to the number of incident protons. Beam intensities were determined during each run by measuring elastically scattered protons with calibrated scintillators. In the case of the two higher beam momenta, the geometrical acceptance of the spectrometer is truncated in the horizontal direction by the side yokes of the dipole magnets. To correct for these losses the following procedure was followed: each event in the c.m. distribution was expressed as function of the azimuthal and the cosine of the polar scattering angle, transforming the spherical surface area into a rectangular area. Required acceptance corrections on the c.m. momentum distribution were based on events missing from such a rectangular shaped density distribution. Measured differential cross section angular distributions are shown in Fig. 2 at the five different beam momenta, each indicated in terms of the corresponding value of η. It is found that the angular distributions become flatter as the beam momentum decreases. As the measured cross sections cover between 75% (800.5 MeV/c) and 100% of the c.m. angular scattering range, the extraction of S– and P–wave contributions to the cross sections is facilitated. Absolute differential cross sections were fitted using the relation

$$4\pi\frac{d\sigma}{d\Omega} = A_0\mathrm{P}_0[\cos(\theta_{\mathrm{cm}})] + A_2\mathrm{P}_2[cos(\theta_{\mathrm{cm}})]\,, \tag{2}$$

where $\mathrm{P}_l[\cos(\theta_{\mathrm{cm}})]$ denote Legendre polynomials, A_0 the total cross section and A_2 the P–wave contribution to the cross section. The fits to the experimental data are also shown in Fig. 2. Extracted values for A_0 and A_2 are presented in Table I.

TABLE I

Deduced parameters from Eq. (2), measured anisotropies (A_2/A_0), applied Coulomb correction factors, Coulomb corrected experimental total cross sections σ. Errors include statistical errors, uncertainties in the beam intensities (typically 5%), target thickness and a 20% systematic error in A_2 due to the acceptance corrections.

η	A_0 (μb)	A_2 (μb)	A_2/A_0	Coulomb correction	σ (μb)
0.062	8.2±0.4	0.066±0.25	0.008±0.03	0.74	11.1±0.3
0.09	12.9±0.9	1.1±0.6	0.09±0.05	0.79	16.3±1.1
0.13	21.8±1.6	2.7±0.7	0.12±0.03	0.85	25.6±1.9
0.18	28.4±2.1	5.2±1.2	0.18±0.04	0.89	31.9±2.4
0.22	45.7±3.3	13.3±2.7	0.29±0.06	0.91	50.2±3.6

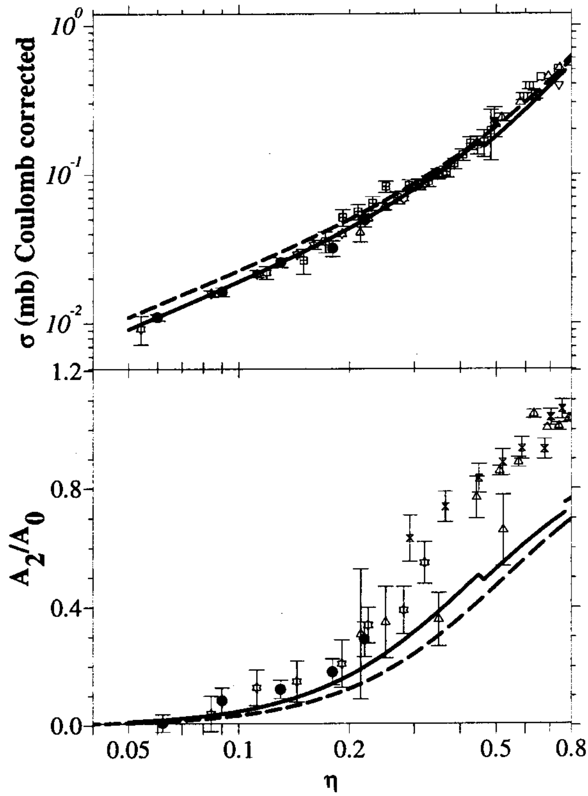

Fig. 3. Upper part: Total cross sections for the $pp \to d\pi^+$ reaction (full circles) as function of η ($p_\pi/m_\pi c$). Also shown are published data for the present reaction (full triangle up [11] and full triangle down [12]), data for the $\pi^+ d \to pp$ reaction assuming time reversal invariance (open circle [13], open square [14], open triangles down [15] up [16], [8], crossed square [5]) and for the $np \to d\pi^0$ reaction assuming isospin symmetry (open star [4]). Corrections to the data are described in the text. Calculations with Eq. (1) using $\alpha_0 = 0.182 \pm 0.006$ (0.22) mb and $\alpha_1 = 0.93 \pm 0.06$ (0.79) mb yield the solid (dashed) curve. Lower part: Measured anisotropies (A_2/A_0) compared with earlier results represented by the same symbols as in the upper part. Additional data of Ref.[20] for the $np \to d\pi^0$ reaction are shown as hourglasses. The curves are calculations with Eq. (3) using the same values of α_0 and α_1 as in the upper part.

To obtain Coulomb–corrected experimental total cross sections, the deduced values of A_0 were divided by appropriate Coulomb suppression factors listed in Table I which were taken from results of Reitan [10] and found to be almost identical for $S-$ and P–wave emission. In Fig. 3 we compare our Coulomb–corrected total cross sections (listed in Table I) to the world data set. Total cross sections for the same reaction are from Refs. [11] and [12] while data from the time–reversed $\pi^+d \to pp$ reaction are taken from Refs. [5, 8, 13–16] and were corrected for in terms of detailed balance. All the selected data taken from reactions with two charged particles in the exit channel were similarly corrected for Coulomb effects. Total cross sections for the $np \to d\pi^0$ reaction [4] also shown in Fig. 3 were multiplied by an isospin coupling factor of 2 due to isospin symmetry.

Our data are in good agreement with the neutron–induced data and are found to reveal a smooth downward trend in the η dependence of existing total cross sections towards threshold. If the Gell–Mann Watson parameterization Eq. (1) is applied with values of $\alpha_0 = 0.22 \pm 0.01$ mb and $\alpha_1 = 0.79 \pm 0.01$ mb, extracted from a fit to the data for $\eta \leq 0.8$ prior to the inclusion of our data, the dashed curve in the upper part of Fig. 3 is obtained. In agreement with previous findings [11, 17] the assumption of using only S– and P–wave pion amplitudes in the present range of η is found to be still valid. In the range of η covered by the present study as well as the $np \to d\pi^0$ data, the parameterization is found to overpredict the data. Including our $pp \to d\pi^+$ data in fitting Eq. (1) to the total cross sections, an unsatisfactory result is obtained with a value of the reduced $\chi^2 = 16.2$. Assuming an energy dependence of α_0 similar to Refs. [18, 19] does not improve the fit significantly. It was found that data for $\eta > 0.5$ contribute most to the large value of χ^2. After excluding the total cross section data for $\eta > 0.5$, a fit is obtained (reduced $\chi^2 = 0.9$) with $\alpha_0 = 0.182 \pm 0.006$ mb and $\alpha_1 = 0.93 \pm 0.06$ mb. The S–wave strength in the total cross section of $\alpha_0 = 0.182 \pm 0.006$ mb is in perfect agreement with the value of $\alpha_0 = 0.184 \pm 0.005$ mb obtained by Hutcheon *et al.* [4] but substantially lower than the values of 0.240 ± 0.005 mb [5] and 0.247 ± 0.017 mb [18] extracted from charged–particle pion absorption measurements. The extracted P–wave contribution of $\alpha_1 = 0.781 \pm 0.079$ mb [4] is found to agree with the present analysis to within two standard deviations.

Anisotropies (A_2/A_0) as obtained from the Legendre polynomial fits of which the coefficients are listed in Table I, are shown in the lower part of Fig. 3. These values are compared to other data for the same reaction [11], from the time–reversed reaction [8, 16] and the isospin related reaction [4, 20]. This comparison indicates a smooth η dependence. The measured anisotropies are also compared with results from a calculation derived from Eq. (1) as

$$A_2/A_0 = (\alpha_1)/(\alpha_0 + \alpha_1\eta^2) \tag{3}$$

and are shown as curves in the lower part of Fig. 3. The solid curve represents the calculation performed with the presently deduced values of α_0 $= 0.182$ and $\alpha_1 = 0.93$ while the dashed curve is obtained with the results from the fit excluding our data ($\alpha_0 = 0.22$ and $\alpha_1 = 0.79$.) Both curves are found to underpredict the measured anisotropies even in the region of the present study. Such a discrepancy can be understood in terms of a possible interference between the S– and D–wave protons in the pp channel, not accounted for in the phenomenology of Eq. (1) [7]. Reasonable agreement in the present range suggests that the entrance S–wave amplitude near threshold is rather small, which is consistent with previous findings [19, 21, 22].

5. Summary

We have measured full angular distributions and total cross sections for the $pp \to d\pi^+$ reaction between $\eta = 0.062$ and $\eta = 0.22$ which are the first measurements for this reaction at these energies. Making use of a magnetic spectrometer together with a thin target and a small beam emittance, we were able to reconstruct the deuteron momenta at the target from the measured tracks in the focal plane. Coulomb–corrected total cross sections are found to be consistent with results from the time–reversed reactions as well as from the isospin related reaction. The deduced S–wave contribution to the cross section at threshold is $\alpha_0 = 0.182 \pm 0.006$ mb which is smaller than the previous estimates of between 0.2 and 0.3 mb for this reaction but in good agreement with recent results obtained from the isospin related reaction. The corresponding P–wave strength is found to be $\alpha_1 = 0.93 \pm 0.06$ mb. Values obtained for the anisotropy are also found to be consistent with the existing η dependence as revealed by the other relevant data. Calculated values of the anisotropies close to threshold suggest smaller partial S–wave amplitudes in the initial pp system. In the region of larger η, the increasing discrepancies are related to the interferences between the partial S– and D–wave amplitudes in the entrance channel leading to P–wave pion production. Present measured anisotropies indicate that the P–wave contribution to pion production at $\eta = 0.22$ is still $\sim$ 30%, decreasing smoothly down to 0% towards threshold. Comparisons of the present data with previous results support the validity of isospin symmetry and time reversal invariance in the pionic sector.

REFERENCES

[1] C.J. Horowitz, *Phys. Rev.* **C48**, 2920 (1993).
[2] C.J. Horowitz, H.O. Meyer, D.K. Griegel, *Phys. Rev.* **C49**, 1337 (1994).
[3] T.S. H. Lee, D.O. Riska, *Phys. Rev. Lett.* **70**, 2237 (1993).
[4] D.A. Hutcheon *et al.*, *Phys. Rev. Lett.* **64**, 176 (1990).

[5] C.M. Rose, *Phys. Rev.* **154**, 1305 (1967).
[6] J.A. Niskanen, *Phys. Rev.* **C53**, 526 (1996).
[7] M. Gell-Mann, K.M. Watson, *Ann. Rev. Nucl. Sci.* **4**, 219 (1954).
[8] B.G. Ritchie *et al.*, *Phys. Rev. Lett.* **66**, 568 (1991) and *Phys. Rev.* **C47**, 21 (1993).
[9] V. Jaeckle, K. Kilian, H. Machner, C. Nake, W. Oelert, P. Turek, *Nucl. Instrum. Methods* **A 349**, 15 (1994).
[10] A. Reitan, *Nucl.Phys.* **B11**, 170 (1969).
[11] D. Aebischer *et al.*, *Nucl.Phys.* **B108**, 214 (1976).
[12] F. Shimizu *et al.*, *Nucl.Phys.* **A386**, 571 (1982).
[13] D. Axen *et al.*, *Nucl.Phys.* **A256**, 387 (1976).
[14] S.I. Gogolev *et al.*, *Phys. Lett.* **B300**, 24 (1993).
[15] B.M. Preedom *et al.*, *Phys. Lett.* **B65**, 31 (1976).
[16] B.G. Ritchie *et al.*, *Phys. Rev.* **C24**, 552 (1981).
[17] C. Richard-Serre *et al.*, *Nucl.Phys.* **B20**, 413 (1970).
[18] J. Spuller and D.F. Measday, *Phys. Rev.* **D12**, 3550 (1975).
[19] D. Bugg, *J. Phys. G* **10**, 46 1984.
[20] E. Roessle *et al.*, in Pion Production and Absorption in Nuclei - 1981, *AIP Conf. Proc.* **79**, 171 (1982).
[21] B. Blankleider, Ph. D. thesis, Flinders University (1980).
[22] B. Blankleider, I.R. Afnan, *Phys. Rev.* **C31**, 1380 (1985).